The effect of charge compensation through alkali metal co-doping on the luminescence behaviour of $SrAl_4O_7:Sm^{3+}$ phosphor

M. Puchalska*, E. Zych

Faculty of Chemistry, University of Wroclaw, 14. F. Joliot-Curie Street, 50-383 Wroclaw, Poland

A B S T R A C T

A comparative study of the luminescent properties of singly Sm^{3+}-doped and Sm^{3+},Na^+ co-doped strontium aluminates: $Sr_{1-x}Sm_xAl_4O_7$ and $Sr_{1-2x}Sm_xNa_xAl_4O_7$ (x = 0.001–0.1), as a function of activator concentration at room and low (77 K, 16 K) temperature is reported. Upon an excitation at 402 nm all samples exhibit intensive orange-red emission due to the characteristic 4f-4f Sm^{3+} transitions with maximum located at around 598.7 nm. It was found that luminescence properties of both series of materials differ significantly. In $SrAl_4O_7:Sm^{3+}$ at least four distinct activator symmetry sites were identified, which is due to presence of charge compensating defects in the crystal lattice and tendency to form Sm pairs. Charge compensation through alkali metal co-doping led to a smaller perturbation of the local environment symmetry of Sm^{3+} ions and significantly enhanced luminescence intensity. In $SrAl_4O_7:Sm^{3+}$,Na^+ only two of the four non-equivalent centers of Sm^{3+} were found. One of them corresponds to isolated Sm^{3+} ion occupying basically undistorted Sr^{2+} symmetry site offered by host lattice but the other is associated with Sm^{3+} ions forming pairs. Analysis of the luminescence decay traces of both types of materials showed a decreasing decay time constant with rising activator concentration what was mainly attributed to cross-relaxation processes between Sm^{3+} ions. This effect was slightly more pronounced for the Sm^{3+},Na^+ co-doped series due to higher population of Sm^{3+} pairs. Fitting of the $^4G_{5/2}$ state fluorescence decay to the Inokuti–Hirayama model indicated different dominant mechanisms of the self-quenching luminescence of Sm^{3+} in $SrAl_4O_7:Sm^{3+}$ and $SrAl_4O_7:Sm^{3+}$,Na^+, respectively, dipole-quadrupole interaction and dipole–dipole interaction.

1. Introduction

The phase diagram of binary $SrO \cdot Al_2O_3$ system has been determined as consisting of five primary crystalline compounds: $SrAl_2O_4$ ($SrO \cdot Al_2O_3$), $SrAl_4O_7$ ($SrO \cdot 2Al_2O_3$), $SrAl_{12}O_{19}$ ($SrO \cdot 6Al_2O_3$), $Sr_3Al_2O_6$ ($3SrO \cdot Al_2O_3$) and $Sr_4Al_{14}O_{25}$ ($4SrO \cdot 7Al_2O_3$) [1,2]. All these compositions are of interest in industry because of their use for hydraulic cements, laser matrices and long-duration photoluminescence or thermoluminescence pigments [3–12]. Other potential applications of these include photocatalysts [13–15], oxygen sensing materials [8,16] and dense electrochemical membranes with mixed ionic–electronic conductivity for oxygen separation and partial oxidation of methane [17,18]. Strontium aluminates are desirable host materials for rare-earth doped phosphors due to their excellent mechanical and thermal properties combined with high chemical inertness. The most extensively investigated systems are $SrAl_2O_4$, $SrAl_4O_7$, and $Sr_4Al_{14}O_{25}$ activated with Eu^{2+} and Dy^{3+} ions, which were found to exhibit bright long persistence of phosphorescence attractive for application in optical storage media and lighting devices [19–24].

$SrAl_4O_7$ exists in two polymorphs, the α-phase being stable at standard pressure and the β-phase, which can only be synthesized at a high pressure and temperature [3]. α-$SrAl_4O_7$ crystallizes in the monoclinic $CaAl_4O_7$ grossite structure with $C2/c$ space group [25]. Its structure is based upon a framework of AlO_4 tetrahedra. Some of the oxygen atoms are shared between two tetrahedra and the rest of them are distributed between the three ones. The existence of so-called "triclusters" consisting of an oxygen atom surrounded by three Al tetrahedra is very interesting unique feature of the grossite structure. In the crystal lattice Sr^{2+} ions occupy single 5-fold coordinate site with C_2 symmetry, whereas Al^{3+} ions are distributed over two symmetrically independent tetrahedral sites, whose surroundings are quite distorted giving C_1 site symmetry. Several studies have been recently published describing the optical properties of lanthanide and transition metal ions in this host [19–24,26–30]. Most of the research focused on $SrAl_4O_7:Eu^{2+},RE^{3+}$ ($RE^{3+} = Dy^{3+}, Eu^{3+}$) which exhibit long-lasting green phosphorescence [19–24]. It was also shown, that $SrAl_4O_7$ serves as good host materials for trivalent lanthanide ions (Sm^{3+}, Dy^{3+}), which produce narrow emission lines due to intraconfigurational 4-4f

transitions [26]. Yb^{3+}-sensitized upconversion luminescence of Tm^{3+} and Tb^{3+} in this host has been also reported [27,28]. $SrAl_4O_7$ activated with transition metal ions (Cu^+, Mn^{4+}) have also been reported as potential phosphor candidates for white LEDs [29,30].

Recently, the interest in using Sm^{3+} ions as the dopant has increased due to the development of GaN laser diodes at 405 nm that can excite efficiently the visible Sm^{3+} emission. Sm^{3+} ions exhibit intensive orange-red luminescence, due to transitions from the $^4G_{5/2}$ excited electronic state, and producing sharp lines characteristic of f–f transitions. Such luminescence, potentially useful in solid state lighting, has been observed when the ions are doped into various materials, including glasses [31,32], single crystals [33,34], polycrystalline materials [35,36], nanocrystalline powders [37,38] and thin films [39].

The purpose of the present paper is to perform comparative studies of luminescence behaviour of Sm^{3+} doped and Sm^{3+},Na^+ co-doped $SrAl_4O_7$ as a function of activator concentration. The effect of charge compensation through alkali metal co-doping on the structure, excitation and emission spectra as well as the luminescence decay kinetics is analyzed and discussed.

2. Experimental

2.1. Synthesis of phosphor powders

Polycrystalline samples of strontium aluminates activated with Sm^{3+}: $Sr_{1-x}Sm_xAl_4O_7$ and $Sr_{1-2x}Sm_xNa_xAl_4O_7$ (x = 0.001–0.1) as well as $Sr_{1-x}Sm_{2/3 \times}\square_{1/3x}Al_4O_7$ ($\square$ – Sr-vacancy x = 0.03) were synthesized by a Pechini method, similarly as it was described in [27,40]. The starting materials for synthesis were: $Al(NO_3)_3 \cdot 9H_2O$ (99%), $Sr(NO_3)_2$ (99%), $Sm(NO_3)_3 \cdot 6H_2O$ (99.999%), $NaNO_3$ (99.9%), citric acid (CA) and ethylene glycol (EG). The molar ratio of the sum of metal cations (Al^{3+}, Sr^{2+}, Eu^{3+}, Na^+), CA and EG was 1:2:8. First, CA was dissolved in EG, followed by the addition of stoichiometric amounts of metal nitrates. The obtained mixtures were adjusted to pH = 7 by adding the ammonia solution (25%) and next slowly evaporated on a hot plate at ~ 100°C to form a viscous gel. The viscous mass was further heated at 150 °C, what led to esterification process. Afterwards, the solid resins were gradually heated up to 600 °C to obtain raw brownish (due to residual carbon) powders. Finally, these materials were placed in alumina crucibles and calcined according to the following schedule: (1) a heating rate of 5 °C/min from room temperature to 300 °C, (2) a heating rate of 2 °C/min from 300 °C to 500 °C, (3) keeping the temperature of 500 °C for two hours, (4) increasing the temperature up to 1100 °C at a heating rate of 5 °C/min, (5) keeping the temperature of 1100 °C for two hours, (6) cooling in the furnace to room temperature.

2.2. Characterization

The resulting products were pulverized using an agate mortar and pestle. Powder X-ray diffraction (XRD) patterns were measured on a Bruker D8 Advance Diffractometer, by using nickel-filtered Cu $K_{\alpha 1}$ radiation (λ = 1.540596 Å). The measurements were performed for 2θ ranging from 10 to 70° with the 0.016° step.

Photoluminescence excitation and emission spectra were measured at room and liquid nitrogen (77 K) temperatures using a SpectraPro 750 1-meter monochromator coupled to a Hamamatsu R928 photo-multiplier and equipped with a 1200 l/mm grating blazed at 500 nm. A 450 W xenon lamp was used as an excitation source. It was coupled to 275 mm excitation monochromator equipped with a 1800 l/mm grating blazed at 250 nm.

The luminescence decay traces were recorded using a FLS980 spectrofluorimeter (Edinburgh Instruments Ltd.) equipped with a microsecond Xenon flash lamp (μF2) and a red-sensitive photomultiplier (Hamamatsu R-928P) operating within the 200–870 nm range of wavelengths.

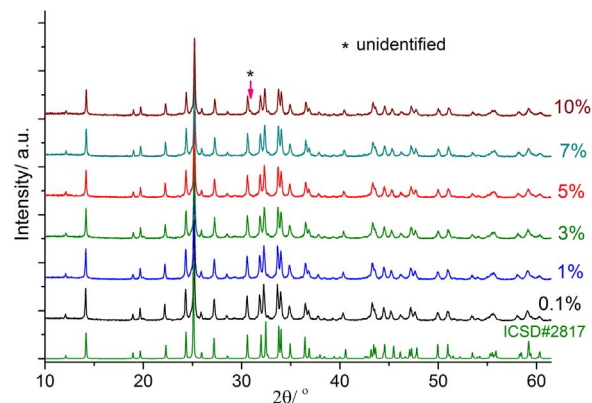Low temperature emission and excitation spectra (16 K) were also

Fig. 1. XRD patterns of the $SrAl_4O_7$:Sm^{3+} samples.

measured on the FLS980 by using an ARS closed-cycle cryostat.

3. Results and discussion

3.1. Structural characterization

Powder XRD patterns of all Sm^{3+} doped and Sm^{3+},Na^+ co-doped $SrAl_4O_7$ are presented in Figs. 1 and 2, respectively. All observed peaks could be indexed using the grossite monoclinic structure of $SrAl_4O_7$, space group $C2/c$, with a = 13.0389 Å, b = 9.0113 Å, c = 5.5358 Å, β = 106.7° and Z = 4 (ICSD file 2817) [25]. In $SrAl_4O_7$ lattice Sr^{2+} ions occupy single site with C_2 (pseudo C_{2v}) symmetry, whereas Al^{3+} ions are distributed over two symmetrically independent tetrahedral sites with C_1 symmetry. Both types of materials are phase-pure in the range of 0.1–7% Sm^{3+} concentration indicating a complete incorporation of dopants in the lattice, while the samples of the highest dopant content (10%) show an additional weak diffraction peak at about 31° 2θ (unidentified) indicating a trace of a foreign phase. The luminescent center, Sm^{3+} ion (r = 1.02 Å), is expected to substitute Sr^{2+} (r = 1.18 Å) rather than Al^{3+} (r = 0.39 Å) due to a much smaller difference in ionic radii [41]. Although in $SrAl_4O_7$ lattice Sr^{2+} ions occupy single crystallographic site, more than one Sm^{3+} sites is expected, because Sm^{3+} - the aliovalent activator – requires a kind of charge compensation to maintain the electrical neutrality of the system. Four possible reaction schemes for charge compensation can be considered and the main difference between them is the type of charge compensating defect involved. Scheme (I) involves compensation by creation of Sr-vacancy, scheme (II) considers the possibility of a Sr^{2+} ion displaced to an Al^{3+} site, scheme (III) involves compensation by creation of interstitials O^{2-} (one interstitial per two dopant ions) and in scheme (IV) one Al-vacancy compensates three trivalent dopants substituting at the Sr^{2+} site. In addition, each charge-compensation
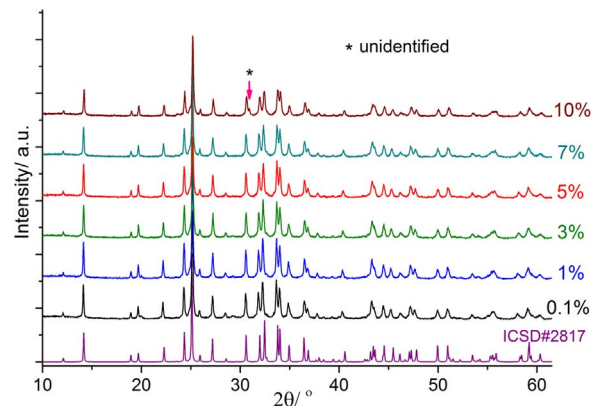

Fig. 2. XRD patterns of the $SrAl_4O_7$:Sm^{3+},Na^+ samples.